This is the peer-reviewed, final accepted version for American Mineralogist, published by the Mineralogical Society of America.
The published version is subject to change. Cite as Authors (Year) Title. American Mineralogist, in press.
DOI: https://doi.org/10.2138/am-2021-7855. http://www.minsocam.org/

Revision 2

Word count: 8.188 abstract and body text only

A RAYLEIGH MODEL OF CESIUM FRACTIONATION IN GRANITE-PEGMATITE SYSTEMS

David London, dlondon1@memphis.edu

Department of Earth Sciences, The University of Memphis, 109 Johnson Hall, Memphis, TN 38152

Abstract

The K/Cs ratios of K-feldspars from granitic pegmatites are compared to models derived from the Rayleigh equation. The K/Cs and K/Rb ratios of K-feldspars and micas exhibit decreasing values when plotted against their Cs or Rb contents across cogenetic suites of granites and pegmatites, and from margin to core of individual bodies. The trends in elemental ratios conform to Rayleigh fractionation for the crystallization of feldspars and micas from a silicate melt. Within two individual pegmatite bodies, the K/Cs ratio of K-feldspar initially falls more rapidly than the Rayleigh model predicts. That might reflect a local increase in the concentration of Cs relative to K due to the pile-up of incompatible elements in a boundary layer of melt adjacent to the crystal growth front. The addition of an aqueous solution to the Rayleigh model (i.e., the simultaneous crystallization of K-feldspars from melt and from aqueous solution) predicts high and increasing K/Cs ratios of K-feldspars that are not observed in natural rock suites, except when K-feldspars crystallize in miarolitic cavities or when primary K-feldspar recrystallizes to microcline perthite in an open hydrothermal system. In those cases, the Cs content of K-feldspars falls to nil because of the high solubility of Cs in aqueous solution and low compatibility of Cs in K-feldspar. Otherwise, the observed patterns of K/Rb or K/Cs in K-

feldspar and micas in pegmatites conform to crystal-melt fractionation in which an aqueous solution plays no part. From the viewpoint of the geochemistry of Cs in pegmatites, these observations give support to the model proposed by Cameron et al. (1949) and endorsed by Jahns (1953a,b).

Key words: cesium, Rayleigh fractionation, pegmatite, K-feldspar

Introduction

Ever since early work by Černý (e.g., Černý et al., 1985), the K/Rb and K/Cs ratios of K-feldspars (reported as a ratio of weight) and of micas have been widely used as monitors of the extent of fractional crystallization of granites and the pegmatites they produce. When graphed as K/Rb versus Rb, K/Rb versus Cs, or K/Cs versus Cs, the resultant patterns exhibit exponentially decreasing trends (e.g., Roda-Robles et al., 2011; Hulsbosch et al. 2014, Marchal et al., 2014, Brown et al., 2017), or decreasing linear arrays in log-log plots (Černý et al., 1985).

Shearer et al. (1992) utilized the K, Rb, Ba, and Cs contents of K-feldspar samples from Harney Peak granite and surrounding pegmatites and compared a Rayleigh model to the fractionation trends across the pegmatite district. Their results are mostly compatible with Rayleigh fractionation, though they note that the rare-element pegmatites are displaced from the trends in trace-element content that link the Harney Peak granite to the tens of thousands of common pegmatites that emanate from it. Kontak and Martin (1997) observed that trace-element variations in K-feldspar from the South Mountain batholith, Nova Scotia, closely fit modeled Rayleigh fractionation trends, though the results for Cs in K-feldspar were erratic. They attributed this variability to the volatility of Cs in an aqueous solution (Carron and Lagache,

1980), implying that the scatter of data reflected variable degrees of recrystallization of the primary K-feldspar and loss of Cs in an open hydrothermal system. Roda-Robles et al. (2012) demonstated that the K/Rb and K/Cs ratios of K-feldspars and micas in the granite-pegmatite system of Pinilla de Fermoselle, Spain, conform to a Rayleigh fractionation trend. Hulsbosch et al. (2014) plotted their analytical data for a field of pegmatites in Rwanda against modeled curves calculated by the Rayleigh equation, and they concluded that the good fit between modeled and actual values was evidence that the crystallization of K-feldspar from melt followed a Rayleigh fractionation process (Figure 1). London et al. (2012, 2020a) likened the pattern of K/Cs in K-feldspar versus distance from pegmatite margin to core to a Rayleigh fractionation process. London et al. (2012, 2020a) observed outliers with anomalously high K/Cs ratios that were attributed to the recrystallization of K-feldspar in an open hydrothermal system.

In their summary of pegmatite geology, Cameron et al. (1949) concluded that zoned pegmatite bodies crystallize from their margins to center as essentially closed systems. If that zonation is fully symmetrical about the central plane of the body, then the distance from margin ($F = 1$ in the Rayleigh equation) to center ($F = 0$) is a proxy for the fraction of melt (F) that has crystallized, or 1-F, in the Rayleigh equation. For this reason, the fraction of melt crystallized, 1-F, is plotted in the figures presented here where values of K/Cs of K-feldspar are normalized to 1-F based on their distance from margin to center.

In these few studies to date, the Rayleigh models and their close correspondence to observed trace-element patterns in K-feldspar apply only to fractionation between minerals and melt, because the partition coefficients utilized are derived from natural or experimental mineral-melt systems. The effects of a coexisting aqueous solution on the K/Cs ratio of K-feldspar have not been considered.

This is the peer-reviewed, final accepted version for American Mineralogist, published by the Mineralogical Society of America.
The published version is subject to change. Cite as Authors (Year) Title. American Mineralogist, in press.
DOI: https://doi.org/10.2138/am-2021-7855. http://www.minsocam.org/

Goals and applications

The goal of this study is to utilize the Rayleigh equation more fully, and specifically to consider the consequences of the separation of an aqueous solution from melt on the K/Cs ratio of K-feldspar at any stage in the formation of a pegmatite body or a pegmatite group. This study models the evolution of the K/Cs ratios of melt, with and without aqueous solution equilibrated with the melt, and of K-feldspar (Kfs) crystallized from the melt only, from the melt in equilibrium with an exsolving aqueous solution, and from an aqueous solution that has exsolved from the melt. The form of the equation used is $C_i = C_o * F^{(D-1)}$, where C_i is the concentration of the trace element *i* in melt, C_o is the initial concentration of that element at the onset of crystallization (F = 1), F is the fraction of melt remaining, and D is bulk distribution coefficient for that element in the crystallizing assemblage.

The results of this study apply to two contrasting models for the internal evolution of pegmatite bodies: the essentially igneous model of Cameron et al. (1949) and the fundamentally aqueous model of Jahns and Burnham (1969). The models are different in another respect: Cameron et al. (1949) advocated a model of sequential fractional crystallization, which included the precipitation of pure quartz cores, the last primary unit to form in common granitic pegmatites, directly from a pegmatite-forming melt. Jahns and Burnham (1969, Jahns, 1982) fit pegmatite consolidation to a model of mineral-melt equilibrium that entailed the simultaneous crystallization of all major minerals in their eutectic proportions in the hydrous granite system. As an economic application, the utility of the K/Cs ratio of K-feldspars to exploration for rare-element deposits in pegmatites is also assessed here. Among those ores, pollucite, nominally $CsAlSi_2O_6$, is highly sought today.

Background

This is the peer-reviewed, final accepted version for American Mineralogist, published by the Mineralogical Society of America.
The published version is subject to change. Cite as Authors (Year) Title. American Mineralogist, in press.
DOI: https://doi.org/10.2138/am-2021-7855. http://www.minsocam.org/

Because of its large ionic radius (mean 1.88 Å with a coordination number of 12: Shannon, 1976) and low charge (+1), Cs is one of the most incompatible elements (incompatibility defined as $C_i^{xl}/C_i^{melt} = D_i^{xl/melt} < 1$) in all of the common rock-forming minerals, including those in which potassium is an essential structural constituent (e.g., London, 2005). Partition coefficients for Cs between the common rock-forming minerals of granites and pegmatites (quartz, sodic plagioclase, K-feldspar, muscovite, and biotite) and their granitic liquids (melt) have been measured (e.g., Table 10-2 of London, 2008, and sources therein), and all are less than unity. It is feasible, therefore, to calculate a bulk distribution coefficient, $D_{Cs}^{xls/melt}$, for the purposes of Rayleigh modeling that is applicable to the crystallization of typical "two-mica" (biotite-muscovite) granites and the pegmatites they spawn (Table 1).

There are few reported values of $D_{Cs}^{Kfs/melt}$ because of the very low concentrations of Cs in K-feldspar and hence the difficulty of measuring it. Icenhower and London (1996) cite $D_{Cs}^{Kfs/melt} = 0.13$ for K-feldspar synthesized from peraluminous rhyolitic melt. Partitition coefficients for sanidine-glass pairs from natural peraluminous rhyolite vitrophyres range from 0.02-0.24 with a mean (n = 12) of 0.16 (Ren, 2004). Nash and Crecraft (1985) reported comparable values (0.11-0.16) for another peraluminous rhyolite. The single value of $D_{Cs}^{Kfs/melt} = 0.13$ is employed for this model.

Cesium is highly compatible in silica-rich melts (e.g., Roy and Navrotsky, 1984), where it can accumulate to weight-percent levels before achieving saturation in pollucite (London et al., 1998), the only significant and rare Cs mineral. Because of the incompatibility of Cs in minerals and the high solubility of pollucite at liquidus temperatures, Cs remains unbuffered to any appreciable extent throughout the fractional crystallization of granite-pegmatite bodies, whereas the K component of melt is constrained to a nearly constant value by the near-eutectic

This is the peer-reviewed, final accepted version for American Mineralogist, published by the Mineralogical Society of America.
The published version is subject to change. Cite as Authors (Year) Title. American Mineralogist, in press.
DOI: https://doi.org/10.2138/am-2021-7855. http://www.minsocam.org/

compositions of the granitic liquids. As a result, the K/Cs ratio of melt decreases over the course of fractional crystallization. The same is true of the principal K-bearing minerals, K-feldspar and micas, in the proportion of their crystal-melt partition coefficients.

Cesium is exceedingly incompatible in K-feldspar in equilibrium with a saline aqueous solution (aq) at elevated pressure and temperature. Values of $D_{Cs}^{aq/Kfs} = 40$ come from two relevant experimental studies (Volfinger, 1969, Carron and Lagache, 1980). Because of its incompatibility in minerals, cesium is also widely regarded as a volatile component in aqueous solutions that might coexist with granitic liquid, but confirming data from experimental measurements are sparse. Two sources that utilized different flux-bearing high-silica liquids at moderate pressures (200 MPa) and temperatures (650°-800°C) yielded similar values, $D_{Cs}^{aq/melt} \approx 0.2$, at < 0.2 molal Cl salinity of the aqueous solution (London et al., 1988, Webster et al. 1989). Even in solutions of such low ionic strength, $D_{Cs}^{aq/melt}$ is twice the value as for K. Values of $D_{Cs}^{aq/melt}$ rise rapidly with increasing chloride salinity of solution, from $D_{Cs}^{aq/melt} = 2.3$ at 2.0 molal Cl to ~ 4-7 at 3-7 molal Cl (Webster et al., 1989). For the purposes of this model, two values of $D_{Cs}^{aq/melt} = 0.2$ and 6.0 illustrate the Rayleigh trends when Cs is highly compatible or highly incompatible in silicate liquid relative to aqueous solution.

Methods of this study

Numerical modeling

A necessary condition for applying the Rayleigh equation is that equilibrium exists among melt, aqueous solution, and the surfaces of crystals, such that the chemical potential gradients of all components, including isotopes, throughout the fluid media are zero. That condition is mandated by the reliance on partition coefficients that are, or are meant to be, as close to the equilibrium of the liquidus as is possible, and by constancy of partition coefficients anywhere in

the system. In order for that to be the case, the diffusivity of all ions through a fluid medium must be rapid in relation to the rate of transfer of those ions to another medium, e.g., from melt to crystals or melt to aqueous solution. The diffusivity of ions through aqueous solutions in response to chemical potential gradients at elevated pressure is believed to be nearly instantaneous, though experimental confirmations of this behavior are almost nil (e.g., Ildefonse et al., 1979). The issue pertains to chemical equilibrium between melt and the surfaces of crystals. At their undercooled conditions of crystallization (e.g., Morgan and London, 1999, London et al., 2012, 2020a,b), pegmatite-forming melts possess exceedingly high viscosities on the order of 10^7-10^8 Pa·s (London, 2008). High viscosity correlates with low diffusivity of most elements (e.g., Mungall, 2002), leading to boundary layer pile-up of incompatible elements (when the accumulation of excluded elements in melt due to crystallization exceeds the rate at which they diffuse away from the crystal-melt interface) and transient gradients in their chemical potentials across the melt volume.

One assessment comes from experiments in which the chemical diffusivity of alkali ions has been measured. Acosta-Vigil et al. (2012a) have observed that the diffusivity of Na and K through melts at high temperature (800°C, 200 MPa) is essentially instantaneous in response to gradients in their own compositions or to gradients imposed by other cations with which the alkalis interact. Morgan and London (2005) found that the diffusion of Na and K through undercooled granitic melt or glass was instantaneous (i.e., equilibrated with aqueous solution and crystals at least on the scale of minutes) down to 515°C at 200 MPa. In a comparison of crystal-melt partitioning in natural glass-mineral pairs, Acosta-Vigil et al. (2012b) ascertained that the distributions of the alkalis, including Cs, came closest of all elements to their published

equilibrium partition coefficients. These results would justify a Rayleigh model for alkalis in natural granite-pegmatite systems.

However, the diffusivity of Cs through melt is the lowest of all the alkali ions, which Roselieb and Jambon (1997) attribute to the large ionic radius of Cs. London and Morgan (2012) documented a pronounced boundary-layer pile up of Rb, Cs, and other incompatible ions (B, F) along a crystallization front that was achieved by liquidus undercooling of a hydrous melt that was derived from the Macusani obsidian. In that case, the Cs content of K-feldspar that crystallized from the melt will reflect the elevated concentration of Cs in the boundary layer liquid, not that of the bulk melt (see Smith et al., 1955). The result would be that the K/Cs and K/Rb ratios of the K-feldspars fall more rapidly than the Rayleigh model would predict, but approach the Rayleigh trend toward the end of crystallization as the system reacts toward the equilibrium of the liquidus. For this scenario, the values of K/Cs and K/Rb ratios in K-feldspar might cross over (i.e., exceed) the Rayleigh trend at the end of crystallization as required by the conservation of mass.

The individual partition coefficients for some mineral-fluid pairs change with the composition of the mineral, of the nutrient solution (melt or aqueous), or with temperature. Bulk distribution coefficients may vary as a mineral assemblage evolves. These factors place additional and well-known limitations on the application of the Rayleigh equation to chemically and mineralogically complex systems. Mineral assemblages and mineral compositions, however, change only slightly from the "two-mica" biotite-muscovite granites to their more fractionated pegmatite bodies. Cesium is so incompatible in rock-forming minerals that its partition coefficients are unlikely to vary over the course of cooling and crystallization. It is for these reasons that the K/Cs ratio of K-feldspar offers a useful test of the applicability of the Rayleigh

fractionation model for pegmatites, and a meaningful assessment of the roles of melt and aqueous solution in the internal evolution of granitic pegmatites. The Rayleigh models developed here with their input parameters are available as Electronic Appendix I. Details of the parameters used are given below where appropriate.

New analyses of K/Cs in K-feldspar

A reconnaissance study included here reports the K/Cs ratio of K-feldspars in three subsurface drill intersections from margin to margin across the General Electric Southeast pegmatite on Hodgeon Hill, near Buckfield, Oxford County, Maine. Inclined drill holes intersected the pegmatite at an angle of ~ 45° to the pegmatite contacts at three different depths (Figure 2). A surface adit into the pegmatite to a distance of ~ 20 meters provides wall-to-wall exposure across the dike. The body strikes east-west with a nearly vertical dip and a thickness of ~ 5 meters. Wall zones on both margins consist of massive medium-grained (2-3 cm) granitic pegmatite with minor biotite. A thin and sporadic band of aplite was exposed along the northern contact of the dike. Symmetrical intermediate zones possess strongly unidirectional solidification texture (UST) in which muscovite crystals up to 60 cm in length form linear ribbons oriented perpendicular to the contact. The core margin is marked by an abundance of tourmaline crystals that exhibit UST and expand toward the core. The core consists of blocky white-beige perthitic K-feldspar with interstitial smoky quartz and minor lenses of pure smoky quartz. Mining by Freeman Resources LLC encountered pods of pollucite, each ~ 0.1-0.3 cubic meters in volume, with minor montebrasite ($LiAlPO_4OH$) and Cs-rich beryl along the center line of the pegmatite at approximately every 3 meters of mining distance into the adit. Other than traces of montebrasite and rare lepidolite rims on muscovite at the core, the pegmatite contains no lithium-rich minerals.

This is the peer-reviewed, final accepted version for American Mineralogist, published by the Mineralogical Society of America.
The published version is subject to change. Cite as Authors (Year) Title. American Mineralogist, in press.
DOI: https://doi.org/10.2138/am-2021-7855. http://www.minsocam.org/

The pegmatite was sampled by recovering chip composites on 10-foot (~ 3 meter) intervals of percussion drilling. The recovery method resulted in a thoroughly mixed sample at each interval of collection. Samples of each interval were split and hand-picked for K-feldspar fragments. Each K-feldspar sample consisted of ~ 15-30 fragments weighing ~ 15-230 grams in total. These were submitted for analysis by Actlabs (Ancaster, Ontario, Canada) using their "4 Litho-quant" analytical package. In that 20-sample set, the average feldspar composition is $Or_{61}Ab_{36}An_{02}$, with a uniform phosphorus content of 0.26 ($1\sigma = 0.06$) wt% P_2O_5 (Electronic Appendix II). The standard deviations were 1.1 wt% for Na_2O and 1.7 wt% for K_2O. In contrast, electron microprobe analyses (Electronic Appendix II) that were restricted to the perthitic portions only yielded an average composition of $Or_{93}Ab_{07}An_{00}$ and standard deviations of 0.25 wt% for Na_2O and 0.33 wt% for K_2O (N = 450). Comparison of the two data sets indicates that the hand-picked sample was contaminated to various degrees by admixed albite as accidental grains and as inclusions within perthite, as this is the norm for pegmatitic K-feldspars (London et al. 2020a,b). Therefore, the K/Cs ratios of the feldspars represent a close approximation to their true value in K-feldspar because albite is not a host for either element. The individual concentrations of K and Cs in the hand-picked sample, however, are not representative of K-feldspar.

The K/Cs ratio of K-feldspar crystallized from melt

Granite to pegmatites

The granite-pegmatite system of the model is a "two-mica" muscovite-biotite granite, for which the bulk distribution coefficient for Cs is 0.05 (Table 1 and Electronic Appendix I). The bulk distribution coefficient for K is derived by dividing the wt% K elemental in each end-member mineral by the concentration of K in the melt. That value is 41489 ppm K for a typical

granitic liquid of metasedimentary (S-type) origin (equivalent to the average of 5 wt% K_2O cited by Chappell and White, 2001). The resulting bulk distribution coefficient for K is 0.92, which reflects the nearly invariant composition of crystals and melt for liquids that crystallize close to their eutectic temperatures. For the Rayleigh model, the initial Cs content of melt is 20 ppm. This is high in relation to subduction-related rhyolite obsidians (average 6 ppm Cs: Macdonald et al., 1992), but appropriate for partial melts that are derived from originally muscovite-rich schists (average 23 ppm Cs: Acosta-Vigil et al., 2010).

With these parameters, the Rayleigh equation was run for the evolution of K and for Cs in melt. The K/Cs of melt is the quotient of these two values at each interation of the Rayleigh equation. The Cs content of K-feldspar is 0.13*Cs in melt. The K/Cs ratio of the feldspar is the quotient of a constant K content (119245 ppm K, which corresponds to a typical composition of Or_{85}) divided by the product of the calculated Cs content of the K-feldspar.

Figure 1 is a plot of K/Cs versus Cs of K-feldspar using these modeled parameters. Plotted against that are analyses from the Rwandan pegmatites that were the source data for Figure 2B of Hulsbosch et al. (2014). Despite small differences in the input parameters of initial Cs content, modal mineralogy, and partition coefficients, the correspondence of modeled and actual values affirms that the compositions of K-feldspars in the Rwandan pegmatites closely approached a Rayleigh fractionation trend for crystallization from the melt, as Hulsbosch et al. (2014) concluded.

Within pegmatites

For the pegmatitic system modeled (Table 1, Electronic Appendix I), the bulk distribution coefficient for Cs is 0.05. With a slightly different modal assemblage, the bulk distribution coefficient for K, $D_K^{xls/melt} = 1.01$, the value of unity that follows from eutectic crystallization.

253 The composition of the K-feldspar is adjusted to Or_{90}, which is more representative of
254 pegmatites than of granites. As before, an aqueous solution is not present in the model.
255 Values of K/Cs of K-feldspar come from two thin subhorizontal pegmatites, cited as the
256 Swamp and Phantom dikes, from Ramona, California (London et al., 2012, 2020a). Both dike
257 sections are ~ 40-50 cm across from the footwall contact to or near the center of each dike.
258 Neither dike is visibly miarolitic. Other than feldspars and quartz, the pegmatites contain
259 accessory tourmaline and trace amounts of muscovite and garnet. The average Cs content of the
260 Swamp cross section is 8 ppm Cs. The average Cs of the Phantom cross section is 20 ppm Cs. In
261 the Rayleigh model, however, the initial concentration of Cs in melt is set at 75 ppm to scale the
262 modeled values to those of the actual pegmatites. It is possible that the footwall portions of the
263 dikes do not represent the bulk compositions of the pegmatites because the hanging wall portions
264 along the center line of each dike contain an appreciable fraction of the K-feldspar in each dike
265 (Figure 4 of London et al., 2012). Compositions of garnet and of plagioclase indicate that
266 crystallization up from the footwall preceded and advanced faster than did crystallization down
267 from the hanging wall contact, which explains why the dike center lines are displaced toward the
268 top of these and similar thin, layered pegmatite bodies (Morgan and London, 1999, London et
269 al., 2012). In that case, crystallization from margins to the dike center was more sequential than
270 contemporaneous, and the portions of dikes above and below the center line are not mirror
271 images of one another (e.g., see Figure 26 of London, 2014).
272 In Figure 3, the modeled values for K/Cs of melt and of feldspar as calculated above are
273 plotted along with the K/Cs of K-feldspars from the Swamp and Phantom dikes against the
274 fraction of melt crystallized, which is proportional to the distance from margin to center of each
275 dike on the premise that the dikes are fully crystallized from both margins at their centers. The

This is the peer-reviewed, final accepted version for American Mineralogist, published by the Mineralogical Society of America.
The published version is subject to change. Cite as Authors (Year) Title. American Mineralogist, in press.
DOI: https://doi.org/10.2138/am-2021-7855. http://www.minsocam.org/

plot for the Phantom dike terminates at 1-F = 0.8 because this cross section ended ~ 10 cm short of the true dike center. The K/Cs ratios of K-feldspars in the two dikes initially fall more rapidly than the Rayleigh model predicts. The tails of the curves for the pegmatitic K-feldspars approach the final values of the Rayleigh trend or cross over it.

The K/Cs ratio of K-feldspar crystallized from melt and aqueous solution

The additional effect of an aqueous solution in equilibrium with melt and crystals is modeled as follows. In the Rayleigh model, the initial Cs content of melt is 100 ppm. First, the Rayleigh equation is solved for Cs in melt versus 1-F, wherein the bulk distribution coefficient is the same as $D_{Cs}^{aq/melt}$ (values of 0.2 and 6.0 in this study). In this first step, the value 1-F corresponds to the fraction of aqueous solution in the system of melt-aqueous solution and to the fraction of melt crystallized, as the mass of exsolved aqueous solution increases in response to crystallization of the melt. The resultant values of Cs are those of the melt. The melt composition is then adjusted for the small fraction of Cs that is removed by crystallization. Following this step, the Cs content of the aqueous solution is the product of Cs in melt times the value of $D_{Cs}^{aq/melt}$ (0.2 or 6.0) at each iteration of 1-F in the Rayleigh equation. The K/Cs ratio of K-feldspar crystallized from the melt is the constant K content for Or_{90} (126259 ppm) divided by the Cs concentration in K-feldspar, which is 0.13*Cs in melt. The concentration of Cs in feldspar crystallized from aqueous solution is the product of the Cs content of aqueous solution times the reciprocal of the published partition coefficient (Volfinger, 1969; Carron and Lagache, 1980), i.e., $D_{Cs}^{Kfs/aq} = 0.025$. The elemental K content of the feldspar is again held constant at Or_{90}. The K/Cs ratio of K-feldspar crystallized from aqueous solution is that K value divided by the concentration of Cs. The resultant values are plotted against 1-F as described above. By this sequence of steps, the Rayleigh models simulate the K/Cs ratios of K-feldspars that crystallize

This is the peer-reviewed, final accepted version for American Mineralogist, published by the Mineralogical Society of America.
The published version is subject to change. Cite as Authors (Year) Title. American Mineralogist, in press.
DOI: https://doi.org/10.2138/am-2021-7855. http://www.minsocam.org/

299 simultaneously from melt and from aqueous solution as the fraction of crystallization and the
300 fraction of aqueous solution increase with 1-F.

301 In Figure 4a, the fractionation trend for K/Cs of K-feldspar crystallized from melt in
302 equilibrium with a low-salinity solution and $D_{Cs}^{aq/melt} = 0.2$ is similar in slope and form to the
303 aqueous solution-absent case (e.g., the modeled values in Figure 3) because the loss of Cs to
304 aqueous solution is negligible over the course of crystallization. The K/Cs ratio of K-feldspar
305 crystallized from aqueous solution, however, is exceedingly and unrealistically high in relation to
306 the values that are reported from natural samples in this study and the others cited.

307 In Figure 4b, the K/Cs ratios of K-feldspar crystallized from melt and from aqueous solution
308 of high salinity, with $D_{Cs}^{aq/melt} = 6.0$, increase exponentially as crystallization proceeds. This is
309 because the large partition coefficient, $D_{Cs}^{aq/melt}$, depletes the melt in Cs as the mass fraction of
310 aqueous solution increases. The concentration of Cs in aqueous solution also falls as the mass of
311 that solution increases. The feldspars crystallized from melt or from aqueous solution, therefore,
312 record a progressive increase in their K/Cs ratios, as most of the Cs winds up in the aqueous
313 solution.

314 **Discussion**

315 **The record of K/Cs in pegmatitic K-feldspar**

316 The high incompatibility of Cs in nearly all of the principal rock-forming minerals (except
317 cordierite: Evensen and London, 2003) means that its concentration in partial melts is unbuffered
318 by subsequent crystallization. It is, therefore, a useful diagnostic of the parental source of
319 pegmatites, which are the products of protracted fractional crystallization of larger igneous
320 bodies (e.g., Černý et al. 1985; Černý 1991; London, 2008, 2019). Černý (1991) rightly
321 associated the Cs-rich pegmatites (his LCT family, for Li-Cs-Ta) with granites that are sourced

from previously unmelted metasedimentary rocks, which are mostly marine deposits of black shale and arkosic turbidite. The Cs-enriched signature of this source arises from the adsorption and incorporation of Cs in the micaceous minerals, including clays, sericite, and chlorites (see London, 2016, 2018 and citations therein). Anomalously high concentrations of boron and phosphorus in the LCT family of pegmatites also originate with their inclusion in marine sediments.

Gordiyenko (1971) made the initial observations that the Rb and Cs contents of K-feldspar increase inward within zoned pegmatite dikes. Petr Černý demonstrated that the plot of K/Cs or K/Rb versus Cs of K-feldspars follows an exponentially decreasing trend from the granites to their most evolved and distal rare-element pegmatites (Černý, 1994, Černý et al., 1985). As is evident from this study, that trend is a result of the fractional crystallization of K-feldspar from the melt, and the K-feldspars mostly preserve it faithfully, even as recrystallized perthitic microcline. It is for this reason that London et al. (2012, 2020a,b) concluded that feldspar solvus thermometry can be a valid record of the original temperature of crystallization of primary feldspars once the compositions of the perthitic K-feldspar are properly analyzed and integrated.

To be sure, not all K-feldspars in granites and pegmatites preserve their initial igneous compositions, but the K/Cs ratio and total Cs contents are sensitive monitors of alkali loss in an open hydrothermal system. London et al. (2012a) pointed to outliers (light blue diamonds of Figure 3) of high K/Cs as indicative of feldspars that have lost Cs, and therefore have recrystallized to some extent in an open system. In Figure 3 of Parsons et al. (2009), two populations of alkali feldspar – one with elevated Cs contents, the other with values below detection limits – from the Klokken granite intrusion in South Greenland, reflect their igneous and hydrothermal origins, respectively.

345 The observed patterns of K/Cs and K/Rb in K-feldspar are mirrored by the micas from
346 granites and pegmatites. The partition coefficients for Rb and Cs are nearly identical in K-
347 feldspar and micas over a range of compositions of melt and aqueous solution (Volfinger, 1969).
348 The primary-appearing coarse-grained micas record the same exponentially decreasing K/Rb and
349 K/Cs ratios that reflect their crystallization from silicate liquid in the pegmatites studied to date
350 (e.g., Černý, 2005, Canosa et al. 2007; Roda-Robles et al., 2012; Marchal et al. 2014, Neiva,
351 2014). What holds true for the K-feldspars holds true for the micas, as Hulbosch et al. (2014)
352 demonstrated for K/Rb and K/Cs ratios in primary K-feldspars and micas in pegmatites from
353 Rwanda: they follow Rayleigh fractionation trends for their crystallization from the silicate melt.

354 **An assessment of case studies**

355 Several of the pegmatites mentioned here deserve some discussion. The Tanco pegmatite,
356 Manitoba, is included because it is an archetype of the LCT family of rare-element pegmatites
357 and their associated ores, its feldspars are well studied, and it is essentially flat-lying. The K/Cs
358 data set for the General Electric Southeast pegmatite, Maine, is unique because it spans a vertical
359 pegmatite from border to border. The Swamp and Phantom dikes, California, are among the very
360 few for which K/Cs ratios are available from margin to core, and for which the temperatures of
361 their crystallization are well constrained (London et al., 2012, 2020a). Feldspars that crystallize
362 in miarolitic cavities and that recrystallize with the formation of perthitic microcline bear upon
363 the role of aqueous solutions in the late stages of pegmatite consolidation.

364 **Tanco pegmatite, Manitoba.** On average (Table 2 and Figures 2 and 7B of Brown et al.,
365 2017), blocky K-feldspars in the Tanco pegmatite, Manitoba, exhibit the decrease in K/Cs from
366 border to late units that follows upon chemical fractionation and crystallization from a melt. That
367 trend begins to reverse itself in zone 90 (from K/Cs = 50 to K/Cs = 775, Figure 2c of Brown et

al., 2017), which is dominated by fine-grained lepidolite and is regarded as the last mappable unit to have crystallized in the pegmatite after the pollucite zone 80 (Černý, 2005; Stilling et al. 2006). Brown et al. (2017) identified five textural-paragenetic types of what they term "metasomatic" K-feldspars at Tanco, implying that these feldspars formed by replacement of a previous mineral or mineral assemblage through chemical exchange in an open hydrothermal systerm. Similar generations of chemically complex and heterogeneous late-stage K-feldspar have been described elsewhere (e.g., Teertstra et al. 1999). The "metasomatic" feldspars are fine grained and exceedingly rare. In a few samples, the concentrations of Rb and of Cs in such feldspars are among the highest measured, but most of the reported analyses are below detection levels and reported as zero values (Table 3 of Brown et al., 2017). Their phosphorus contents include a few values similar to those of the primary blocky perthitic microcline found in these and other peraluminous pegmatites, most of which possesses > 0.3 wt% P_2O_5 (London et al., 1990). However, the large majority of the analyses of "metasomatic" feldspars yield undetectable phosphorus, which is also characteristic of K-feldspars from miarolitic cavities in otherwise phosphate-rich pegmatites (London et al., 2012b). Hydrothermal K-feldspar of adularia habit (Type 6 of Brown et al., 2017) in small and rare vugs is extremely depleted in Cs relative to the primary perthitic microcline in the late-forming zones (Černý et al., 1984; Brown et al., 2017). The reversal in the decreasing trend of K/Cs can be explained if some K-feldspar from zone (90), the "metasomatic" feldspars, and adularia in late-stage vugs reflect the imprint of increasing K/Cs that results when the feldspar crystallizes or recrystallizes from an aqueous solution.

General Electric Southeast pegmatite, Maine. The K/Cs ratios of K-feldspars (Figure 2) exhibit increasing fractionation from both margins of the dike to its core, as might be expected from the bilateral symmetry that is evident in the surface adit of the pegmatite. The symmetry of

This is the peer-reviewed, final accepted version for American Mineralogist, published by the Mineralogical Society of America.
The published version is subject to change. Cite as Authors (Year) Title. American Mineralogist, in press.
DOI: https://doi.org/10.2138/am-2021-7855. http://www.minsocam.org/

391 the curves in Figure 2 is consistent with the model proposed by Cameron et al. (1949), wherein
392 crystallization of the melt proceeds more or less simultaneously from both margins to the centers
393 of dikes. Such zonation is typical of steeply dipping pegmatite bodies, which formed a large
394 proportion of the pegmatites studied by Cameron et al. (1949). The study also demonstrated that
395 exploration based on percussion drilling, which is much less costly than core drilling, can
396 recover samples that reflect the spatial chemical variations in pegmatites.

397 **Swamp and Phantom pegmatites, California.** Plots of K/Cs in K-feldspar versus distance
398 from margin to center for the Swamp and the Phantom pegmatites deviate from the Rayleigh
399 model with ratios that are initially lower (more fractionated) than predicted. These might result
400 from the pile-up of Cs in a boundary layer liquid, as has been observed in experiments, leading
401 to lower K/Cs ratios in the feldspars. The K/Cs values of both dikes approach the Rayleigh trend
402 toward the dike centers, which could be interpreted as an approach to crystal-melt equilibrium as
403 crystallization proceeded. The feldspars also evolve from non-perthitic mixed orthoclase-
404 microcline to coarsely perthitic maximum microcline, and from graphic intergrowths to
405 monophase feldspars from margins to core (London et al., 2012, 2020a). The final K-feldspars
406 from the Swamp dike possess slightly higher K/Cs than the Rayleigh model. This is a necessary
407 consequence of the conservation of mass in the pegmatite body, as more Cs was removed,
408 relative to the Rayleigh model, at early stages of crystallization. The trend in the Phantom dike
409 does not cross the Rayleigh plot, but that dike was not fully sampled to its center line.

410 The Rayleigh model also can be utilized to calculate the initial concentration of Cs of the
411 melt that would be necessary to achieve the observed K/Cs ratios of the first-formed K-feldspars
412 if those feldspars crystallized from an aqueous solution rather than a melt. In that case, the bulk
413 distribution coefficient, $D_{Cs}^{xls/aq}$, for Cs is 0.004 (partition coefficients for micas from Volfinger,

1969). With a bulk distribution coefficient that is approximately an order of magnitude lower than that between crystals and melt, the consequent Cs content of melt needed to reproduce the compositions of the initial feldspars in the Swamp and Phantom dikes is ~ 800 ppm Cs, about an order of magnitude greater than the modeled value in Figure 3. Starting with that initial concentration of Cs, and the miniscule value of $D_{Cs}^{xls/aq}$, that melt would reach 2600 ppm Cs, the concentration of Cs in the bulk composition of the pollucite-rich Tanco pegmatite (Stilling et al., 2006), at just 70% of crystallization. Were this case true, a great many of otherwise common pegmatites would contain pollucite. This conclusion is neither plausible nor consistent with the unfractionated compositions of the Swamp and Phantom dikes (Table 2 of London et al., 2012).

The plot of K/Rb in K-feldspar versus distance from margin (1-F) for the Phantom dike (Figure 14 of London et al., 2020a) more closely approaches the quasi-linear plot of a Rayleigh model than does Cs. Two factors might influence this trend: (1) the higher compatibility of Rb compared to Cs in K-feldspar (Icenhower and London, 1996), and (2) the higher diffusivity of Rb compared to Cs in melt (Roselieb and Jambon, 1997).

Miarolitic pegmatites. The Cs content of K-feldspars in miarolitic cavities is practically unstudied. As noted above, K-feldspar of adularia habit in small and rare vugs at Tanco has essentially no Cs (Černý et al., 1984). Miarolitic K-feldspars from two pegmatites in Argentina were at or below a detection threshold that was reported as 0.01 wt% Cs_2O (Černý et al., 2003). A global survey (London et al., 2020b) found the Cs content of K-feldspars from 12 miarolitic pegmatites to lie below detection by electron microprobe analysis (0.05 wt% Cs_2O calculated at 3σ above mean background). This suite includes samples from the pegmatites of the Little Three mine, Ramona, California (the same locality as the Swamp and Phantom dikes), where quartz and topaz from miarolitic cavities contain daughter minerals including pollucite, ramanite

437 ($CsB_5O_6(OH)_4 \cdot 2H_2O$), and an unnamed Cs arsenate (London et al., 2012) in fluid inclusions of
438 low ionic strength (see column Tm_{ice} in Table 10 of London et al., 2012). Other than its
439 occurrence as a daughter mineral within fluid inclusions, pollucite has not been documented in
440 any of those dikes.

441 **Subsolidus recrystallization to perthite.** London et al. (2012, 2020b) noted that although
442 much of the blocky K-feldspar in the southern California pegmatites is perthitic microcline, that
443 recrystallization mostly occurred without the loss of Cs to an aqueous solution. That is not to say
444 that an aqueous solution was not involved in the transformation to perthitic microcline, but that
445 the recrystallization of the original K-feldspar occurred in a closed system in which the mass
446 fraction of aqueous solution to K-feldspar was negligible.

447 Pegmatites retain their original igneous compositions and structures of K-feldspars more
448 faithfully than do granites because pegmatites possess too little thermal mass to circulate
449 aqueous solutions through solidified rock (e.g., Neves and Godinho, 1999; London, 2008),
450 whereas granites can sustain prolonged hydrothermal interaction. The proportionately large
451 population of Cs-depleted feldspars in granite reported by Parsons et al. (2009) and noted by
452 Kontak and Martin (1997) can be understood on this basis. Such Cs-depleted feldspars are rare in
453 pegmatites, except at the latest, miarolitic stage, and where noted as outliers in the overall trend
454 of chemical fractionation of the blocky, primary K-feldspars.

455 The occurrence of Cs-rich aqueous fluid inclusions with Cs-poor feldspars within miarolitic
456 cavities of pegmatites, intense Cs metasomatism adjacent to pollucite-bearing pegmatites
457 (discussed below), and the complete loss of Cs in K-feldspar that has recrystallized in an open
458 hydrothermal environment attest to the high solubility of Cs in aqueous solution (i.e., $D_{Cs}^{aq/melt} >$
459 1, $D_{Cs}^{aq/Kfs} \gg 1$) . To that extent, the evidence indicates that if a pegmatite-forming melt

crystallizes with a coexisting and increasing fraction of aqueous solution, then the K/Cs ratios of all K-feldspars should follow an evolutionary path like that of Figure 4b. It is the reverse of the solely magmatic trend that the primary K-feldspar records.

The K/Cs ratio of K-feldspars as a prospecting tool

Cesium in the form of a Cs-formate solution is in high demand as a component of the dense mud used in deep drilling for petroleum and natural gas (e.g., Sassen et al., 2002). At present, pollucite represents the only commercial source. Even in pollucite-bearing pegmatites, the mineral constitutes less than one volume percent (Stilling et al., 2006). The demand for ore and the rarity of its occurrence creates a rationale to discriminate those few pegmatites that might contain pollucite from the many that do not. The K/Cs ratios of K-feldspars might be one means of assessment.

The K/Cs ratios of K-feldspars associated with the pollucite zone 80 of the Tanco pegmatite cluster close to ~ 50 (Brown et al., 2017). The K/Cs ratios of K-feldspars in the outer zones 10, 20, and 40, are higher, but they mostly span the full range of values from ~ 1600 to 50 (Brown et al., 2017). At the General Electric Southeast pegmatite, all three drilled intersections yield a K/Cs ratio of K-feldspar that is ~ 183-474 at the core of each pegmatite transect. The highest value, 2177, lies at a margin of the dike. These values are about an order of magnitude greater than those from the Tanco pegmatite. Nonetheless, both pegmatites – Tanco and General Electric Southeast – are equally enriched in pollucite (Stilling et al., 2006, and author's unpublished field data). The K/Cs ratios are meaningful, however, only in relation to the K/Cs ratio of K-feldspar in pegmatites that are less fractionated and that lack pollucite. As examples, the K/Cs ratios of K-feldspar at the interior ends of the Swamp and Phantom dike sections are ~ 500 and 2100 respectively.

The Cs concentration that is necessary to saturate hydrous granitic melt in pollucite falls sharply with decreasing temperature (London et al., 1998). This variable – the temperature of crystallization of the pegmatite-forming melt – adds another measure of uncertainty to the significance of the K/Cs ratios of the K-feldspars as indicators of the probability of finding pollucite in a pegmatite body. Though the ratios among K, Rb, and Cs in alkali feldspars and micas point in the direction of increasing fractionation across a pegmatite field or within a body, they are not yet definitive for distinguishing pollucite-bearing pegmatites from those that lack it.

At Tanco, the late-stage feldspars and the ensuing hydrothermal alteration of host rocks point to the involvement of an aqueous solution toward the end of crystallization in the pegmatite, and to high solubility and high mobility of Cs in that aqueous solution. Morgan and London (1987) observed that the metasomatic alteration that surrounds the Tanco body mirrors the distribution of the latest-formed primary units within the pegmatite. They concluded that all of the primary units, including the pollucite bodies, were solidified before the egress of an aqueous solution out of the pegmatite. A pervasive alteration of host metagabbro to Rb- and Cs-rich zinnwaldite is pronounced wherever large masses of pollucite are concentrated in the pegmatite. Cesium concentrations averaged 1.46 wt% Cs_2O in the metasomatic zinnwaldite (Morgan and London, 1987). Approximately 13% of the original Cs content of the pegmatite was conveyed to the adjacent host rocks (Morgan and London, 1989). The late-stage metasomatism of host rocks, which carries the chemical signature of the last-formed mineral assemblages, mirrors the reversal in the K/Cs ratios of the latest, hydrothermal feldspars in the pegmatite (Brown et al., 2017).

An equally large and fractionated pegmatite (Lower Tanco) beneath the main upper one possesses no known pollucite except traces along its western extremity. A broad (10s of meters) and pervasive zone of exceedingly Cs-rich metasomatic dark mica that has replaced metagabbro

extends off the east end of the body. The aqueous solution responsible for the metasomatic alteration emanated from or through a brecciated aplite within the pegmatite. The Lower Tanco pegmatite appears to have achieved H_2O saturation of melt earlier than the upper body, prior to the crystallization of pollucite, with the result that most of the Cs was transferred from the pegmatite to the reactive host rocks. Other examples of intense wallrock metasomatism in which Cs has been conveyed by aqueous solution to host rocks, where is it sequestered by the crystallization of Cs-rich "biotite", are well documented (e.g., Royzenmen et al., 1982). The spatial correlation of an aureole of Cs-rich mica might augur the location of pollucite mineralization more reliably than do the pegmatitic feldspars. Conversely, a large aureole of Cs-rich mica might signify that the loss of Cs is so extensive that pollucite is not likely to be present in the source pegmatite.

Implications

The Rayleigh models presented here, together with the ratios among K, Rb, and Cs in alkali feldspars and micas, have these implications for understanding the internal differentiation of pegmatites:

(1) Variations of K/Rb and K/Cs versus Rb or Cs generally follow Rayleigh fractionation trends for the crystallization of K-bearing minerals from silicate liquid. Both ratios decrease from source granites to their most fractionated pegmatites, and from the margins of pegmatites to their innermost primary unit. The K/Cs ratio of K-feldspar initially decreases more rapidly than the Rayleigh model predicts for two dikes in California (London et al., 2012, 2020a), which can be attributed to the accumulation of Cs relative to K in a boundary layer of liquid along the crystallization front. The K/Cs ratios of those K-feldspars converge on the Rayleigh fractionation trend and one crossed over that trend as crystallization advanced toward the centers of the dikes.

Both results can be interpreted to mean that K-feldspar and melt more closely approached a state of chemical equilibrium as crystallization advanced inward. The textures of the feldspars are consistent with this interpretation.

(2) If Cs is not volatile in a system of melt-aqueous solution (Figure 4a), then the values of K/Cs versus Cs for K-feldspar that crystallizes from the melt are essentially those of the aqueous solution-absent model. In that case, however, K-feldspar that crystallizes simultaneously from a coexisting aqueous solution will have essentially no Cs and exceedingly high K/Cs because of the large partition coefficient, $D_{Cs}^{aq/Kfs}$.

(3) If K-feldspar in the two dikes from California crystallized from melt components via their dissolution into and through an aqueous solution that wetted the surfaces of crystals, then the Cs content of the bulk melt needed to reproduce the K/Cs ratios of the first-formed feldspars are implausibly high.

(4) If Cs is volatile in a system of melt-aqueous solution (Figure 4b), then all K-feldspars, whether crystallized from the melt or from the aqueous solution, will exhibit trends of increasing K/Cs (depletion in Cs) as the small quantity of Cs partitions into an increasing mass of aqueous solution. None of the sources of data for feldspars or micas cited here conforms to this trend, except in the very late stages of pegmatite consolidation when miarolitic cavities form and when subsolidus recrystallization occurs in an open hydrothermal system.

Pegmatite paradigms in the context of Cs geochemistry

Cameron et al. (1949) remains as the most comprehensive and authoritative publication of pegmatite geology, That summary, which included R.H. Jahns as the second author, attributed the internal features of zoned pegmatites to the fractional crystallization of granitic melt from the margins of a body to its center. Their evidence for fractionation crystallization included the

552 highly directional growth of minerals from margins to center and systematic changes in mineral
553 habits and mineral assemblages with position within a pegmatite body. They recognized fracture-
554 controlled replacements of minerals in the outer zones of pegmatites as reactions between early-
555 formed minerals with later, more fractionated melt with which the outer pegmatite zones were
556 not in equilibrium.

557 Cameron et al. (1949) also cited a systematic decrease in the anorthite content of plagioclase
558 (p. 101-102) in support of a fractional crystallization model, but their data were not published.
559 Detailed profiles of the anorthite content of plagioclase with distance from margin to center are
560 now available (London et al., 2012, 2020a), and they bear out all of the trends mentioned by
561 Cameron et al. (1949).

562 Cameron et al. (1949) hypothesized that the increasing size of crystals from margin to center
563 arose from a reduction in the viscosity of the melt as "hyperfusibles" (p. 105) – incompatible
564 components that act as fluxes in the melt – became concentrated in the "rest-liquid". As such,
565 they viewed the giant crystals found in the innermost zones to be the products of crystallization
566 from a melt. Cameron et al. (1949) relegated an aqueous solution to a minor role in the
567 subsolidus alteration of primary minerals, which they and others (e.g., Jahns, 1953b, Heinrich,
568 1953) put at generally less than 1 vol% of any given pegmatite body. Jahns (1953a,b) advocated
569 these conclusions, taking text verbatim from Cameron et al. (1949) in his first academic
570 publications.

571 Jahns (1955) subsequently invoked an aqueous fluid as the principal agent that promoted the
572 formation of pegmatites as opposed to granites. That hypothesis, which was fully presented by
573 Jahns and Burnham (1969; Jahns, 1982), relegated the silicate melt to a mass that was
574 redistributed via diffusion through and buoyant ascent of the aqueous solution. Ever since, the

This is the peer-reviewed, final accepted version for American Mineralogist, published by the Mineralogical Society of America.
The published version is subject to change. Cite as Authors (Year) Title. American Mineralogist, in press.
DOI: https://doi.org/10.2138/am-2021-7855. http://www.minsocam.org/

575 occurrence of pegmatites has been generally regarded as a priori evidence that an aqueous
576 solution has exsolved from an H_2O-saturated granitic liquid, and the pegmatitic stage marks the
577 onset of exsolution of that aqueous solution.[1]

578 Jahns and Burnham (1969; Jahns, 1982, and R.H. Jahns, personal communication, 1982)
579 envisioned that the melt dissolves into an aqueous solution that forms an interconnected and
580 continuous film along crystal surfaces. Chemical fractionation occurs between the melt and
581 aqueous solution, such that the crystals that grow via "*nourishment*" (Jahns and Burnham, 1969,
582 p. 856) from the aqueous solution become progressively enriched in normally rare and
583 incompatible elements (see Figure 2 of Jahns, 1982). This is precisely the scenario that is
584 captured by the Rayleigh models of Figure 4, wherein the aqueous solution might be regarded as
585 an interface between the melt and the crystals that grow from it, whose values of $D_{Cs}^{Kfs/aq}$ are
586 those of the crystal-aqueous solution equilibrium. Those Figures 4a,b indicate that the K/Cs
587 ratios of K-feldspars that crystallize from an aqueous solution will be unrealistically high.
588 Conversely, the Cs concentration of the melt would have to be unrealistically high to reproduce
589 the observed K/Cs ratios of K-feldspars if these were crystallized from the aqueous solution.
590 Rather than enriching K-feldspar in Cs as Jahns and Burnham (1969) envisioned, crystallization
591 from an exsolving aqueous solution would cause depletion of Cs in the K-feldspar.

592 Based on what is evident from field and experimental data, Cs behaves as a volatile
593 component, meaning it is concentrated in aqueous solution over crystals or melt. The Rayleigh
594 modeling presented here shows that if Cs were partitioned in favor of the aqueous solution

[1] Jahns and Burnham (1969) regarded the converse as true: the typical plutonic texture of granite arises from the crystallization of the melt alone in the absence of an aqueous solution. Burnham (1979) proposed a model for the generation of subduction-related base-metal deposits in which an aqueous solution separated early in the crystallization of a granitic magma body, but quartz veins, not pegmatite dikes, were generated in the process. The contradiction between this model and that of Jahns and Burnham (1969) has not been addressed. Černý et al. (2012) observed that pegmatites are absent from these subduction-related base-metal granitoids unless they contained an added fluxing component, such as boron, from marine sediment or altered oceanic crust.

595 ($D_{Cs}^{aq/melt} > 1$), then all feldspars, whether grown from melt or aqueous solution, would become
596 progressively depleted in Cs as crystallization proceeds (Figure 4b). That is not the case: the
597 patterns of K/Rb or K/Cs in the primary, coarsely crystalline K-feldspar and micas in pegmatites
598 conform to crystal-melt fractionation in which an aqueous solution played no part. The negligible
599 Cs contents of K-feldspars that form in miarolitic cavities and by the subsolidus replacement of
600 blocky primary crystals are consistent with feldspar precipitation from an aqueous solution in
601 which Cs is highly compatible and mobile. Those Cs-depleted feldspars, however, appear only in
602 the very latest stages of primary and subsolidus crystallization of pegmatites. From the viewpoint
603 of the geochemistry of Cs in pegmatites, these observations give support to the model proposed
604 by Cameron et al. (1949) and endorsed by Jahns (1953a,b).

605 **Acknowledgements**

606 This study was supported by the National Science Foundation (grant EAR-1623110). Niels
607 Hulsbosch provided data for the Rwandan pegmatites used in Figure 1. Canada Sinomine
608 Resources Inc. permitted the release of unpublished information regarding the Lower Tanco
609 pegmatite body, Manitoba, and analyses of feldspars from the General Electric Southeast
610 pegmatite, Maine. Gary Freeman (Freeman Resources LLC) provided samples, access, and
611 information regarding the pegmatites of Hodgeon Hill, Maine. I thank Mona-Liza Sirbescu,
612 Callum Hetherington, and Cal Barnes for their constructive reviews and Cal Barnes for editorial
613 handling.

614

615 **References**

616 Acosta-Vigil, A., Buick, I., Hermann, J., Cesare, B., Rubatto, D., London, D., and Morgan, G.B.
617 VI. (2010) Mechanisms of crustal anatexis: a geochemical study of partially melted
618 metapelitic enclaves and host dacite, SE Spain. Journal of Petrology, 51, 785-821.
619 Acosta-Vigil, A., Buick, I., Cesare, B., London, D., and Morgan, G.B. VI (2012b) The extent of
620 equilibration between melt and residuum during regional anatexis and its implications for
621 differentiation of the continental crust: a study of partially melted metapelitic enclaves.
622 Journal of Petrology, 53, 1319-1356.
623 Acosta-Vigil, A., London, D., and Morgan, G.B. VI (2012a) Chemical diffusion of major and
624 minor components in granitic liquids: implications for the rates of homogenization of crustal
625 melts. Lithos, 153, 308-323.
626 Brown, J.A., Martins, T., Černý, P. (2017) The Tanco Pegmatite at Bernic Lake, Manitoba.
627 XVII. Mineralogy and geochemistry of alkali feldspars. The Canadian Mineralogist, 55, 483-
628 500.
629 Burnham, C.W (1979) Magmas and hydrothermal fluids. In Geochemistry of hydrothermal ore
630 deposits, 2nd ed. (Barnes, H.L, ed.). John Wiley and Sons, New York, 71-136
631 Cameron, E.N., Jahns, R.H., McNair, A.H., and Page, L.R. (1949) Internal structure of granitic
632 pegmatites. Economic Geology Monograph 2, 115 p.
633 Canosa, F., Martin-Izard, A., and Fuertes-Fuente, M. (2012) Evolved granitic systems as a
634 source of rare element deposits; the Ponte Segade case (Galicia, NW Spain). Lithos, 153,
635 165-176.
636 Carron, J-P. and Lagache, M. (1980) Étude expérimentale du fractionnement des éléments Rb,
637 Cs, Sr, et Ba entre feldspaths alcalins, solutions hydrothermales et liquides silicatés dans le
638 système Q.Ab.Or.H_2O à 2 kbar entere 700 et 800°C. Bulletin de Mineralogie, 103, 571-578.

639 Chappell, B.W., and White, A.J.R. (2001) Two contrasting granite types: 25 years later:
640 Australian Journal of Earth Sciences, 48, 489-499.
641 Černý, P. (1991) Rare-element granite pegmatites. Part I: anatomy and internal evolution of
642 pegmatite deposits. Geoscience Canada 18, 49-67.
643 Černý, P. (1994) Evolution of feldspars in granitic pegmatites. In Feldspars and their reactions
644 (Parsons, I., ed.). NATO Advanced Study Institutes Series C, Mathematical and Physical
645 Sciences, 421, 501-540.
646 Černý, P. (2005) The Tanco rare-element pegmatite deposit, Manitoba: regional context, internal
647 anatomy, and global comparisons. In Rare-Element Geochemistry and Mineral Deposits
648 (R.L. Linnen & I.M. Samson, eds.). Geological Association of Canada Short Course Notes
649 17, 127–158.
650 Černý, P. and Chapman, R. (1984) Paragenesis, chemistry and structural state of adularia from
651 granitic pegmatites. Bulletin de Mineralogie, 107, 369-384.
652 Černý, P., London, D., and Novak, M. (2012) Granitic pegmatites as reflections of their sources.
653 Elements, 8, 257–261.
654 Černý, P. Meintzer, R.E., and Anderson, A.J. (1985) Extreme fractionation in rare-element
655 granitic pegmatites: selected examples of data and mechanisms. Canadian Mineralogist, 23,
656 381-421.
657 Evensen, J.M. and London, D. (2003) Experimental partitioning of Be and other trace elements
658 between cordierite and silicic melt, and the chemical signature of S-type granite.
659 Contributions to Mineralogy and Petrology, 144, 739-757.

660 Gordiyenko, V.V. (1971) Concentrations of Li, Rb, and Cs in potash feldspar and muscovite as
661 criteria for assessing the rare-metal mineralization in granite pegmatites. International
662 Geology Review, 13, 134-142.
663 Heinrich, E.W. (1953) Zoning in pegmatite districts. American Mineralogist, 38, 68-87.
664 Hulsbosch, N., Hertogen, J., Dewaele, S., André, L., and Muchez, P. (2014) Alkali metal and
665 rare earth element evolution of rock-forming minerals from the Gatumba area pegmatites
666 (Rwanda): Quantitative assessment ofcrystal-melt fractionation in the regional zonation of
667 pegmatite groups. Geochimica et Cosmochimica Acta, 132, 349–374.
668 Icenhower, J.P. and London, D. (1996) Experimental partitioning of Rb, Cs, Sr, and Ba between
669 alkali feldspars and peraluminous melt. American Mineralogist, 81, 719-734.
670 Ildefonse, J.P., Jambon , A., Carron , J.P., Delbove, F. and Gabis, V. (1979) La diffusion
671 chimique dans les solutions hydrothermales et dans les verres et magmas silicatés. Sciences
672 Geologiques, Mémoir, 53, 81-85.
673 Jahns, R.H. (1953a) The genesis of pegmatites. I. Occurrence and origin of giant crystals.
674 American Mineralogist, 38, 563-598.
675 Jahns, R.H. (1953b) The genesis of pegmatites. II. Quantitative analysis of lithium bearing
676 pegmatite, Mora County, New Mexico. American Mineralogist, 38, 1078-1112.
677 Jahns, R.H. (1955) The study of pegmatites. Economic Geology, 50th Anniversary Volume,
678 1025-1130.
679 Jahns, R.H. (1982) Internal evolution of pegmatite bodies. Granitic pegmatites in science and
680 industry (Černý, P., ed.). Mineralogical Association of Canada Short Course Handbook, 8,
681 293-327.

682 Jahns, R.H., and Burnham, C.W. (1969) Experimental studies of pegmatite genesis: I. A model
683 for the derivation and crystallization of granitic pegmatites. Economic Geology 64, 843-864.
684 Kontak, D.J. and Martin, R.F. (1997) Alkali feldspar in the peraluminous South Mountain
685 Batholith, Nova Scotia: trace-element data. Canadian Mineralogist, 35, 959-977.
686 London, D. (2005) Geochemistry of alkali and alkaline earth elements in ore-forming granites,
687 pegmatites, and rhyolites. In "Rare-Element Geochemistry of Ore Deposits" (Linnen, R.L.
688 and Sampson, I.M., eds.). Geological Association of Canada Short Course Handbook, 17, 17-
689 43.
690 London, D. (2008) Pegmatites. Canadian Mineralogist Special Publication, 10, 368 p.
691 London, D. (2014) A petrologic assessment of internal zonation in granitic pegmatites. Lithos,
692 184-187, 74-104.
693 London, D. (2016) Rare-element granitic pegmatites, in Rare earth and critical elements in major
694 deposit types (Verplanck, P.L. and Hitzman, M.W., eds). Reviews in Economic Geology,
695 Society of Economic Geologists, Inc, Littleton, CO, 18, 165–193.
696 London, D. (2018) Ore-forming processes within granitic pegmatites. Ore Geology Reviews,
697 101, 349-383.
698 London, D., Černý, P., Loomis, J.L., and Pan, J.J. (1990) Phosphorus in alkali feldspars of rare-
699 element granitic pegmatites. Canadian Mineralogist, 28, 771-786.
700 London, D., Hervig, R.L., and Morgan, G.B., VI (1988) Melt-aqueous solution solubilities and
701 element partitioning in peraluminous granite-pegmatite systems: Experimental results with
702 Macusani glass at 200 MPa. Contributions to Mineralogy and Petrology, 99, 360-373.

London, D., Hunt, L.E., Schwing, C.R., and Guttery, B.M. (2020a) Feldspar thermometry in pegmatites: truth and consequences. Contributions to Mineralogy and Petrology, 175, https://doi.org/10.1007/s00410-019-1617-z.

London, D., Hunt, L.E., Duval, C.L. (2020b) Temperatures and duration of crystallization in gem-bearing granitic pegmatites. Lithos, 360-361, https://doi.org/10.1016/j.lithos.2020.105417.

London, D. and Morgan, G.B. VI (2012) The pegmatite puzzle. Elements, 8, 263–268.

London, D., Morgan, G.B. VI, and Icenhower, J. (1998) Stability and solubility of pollucite in granitic systems at 200 MPa H_2O: Canadian Mineralogist, 36, 497-510.

London, D., Morgan, G.B. VI, Paul, K.A., and Guttery, B.M. (2012) Internal evolution of a miarolitic granitic pegmatite: the Little Three Mine, Ramona, California (USA). Canadian Mineralogist, 50, 1025-1054.

Macdonald, R., Smith, R.L., and Thomas, J.E. (1992) Chemistry of the subalkalic silicic obsidians. U.S. Geological Survey Professional Paper, 1523, 214 p.

Marchal, K., Simmons, W.B., Falster, A.U., Webber, K.L., and Roda-Robles, E, et al. (2014) Geochemistry, mineralogy, and evolution of Li-Al micas and feldspars from the Mount Mica pegmatite, Maine, USA. The Canadian Mineralogist, 52, 221-233.

Morgan, G.B., VI and London, D. (1987) Alteration of amphibolitic wallrocks around the Tanco rare-element pegmatite, Bernic Lake, Manitoba. American Mineralogist, 72, 1097-1121.

Morgan, G.B., VI and London, D. (1989) Experimental reactions of amphibolite with boron-bearing aqueous fluids at 200 MPa: Implications for tourmaline stability and partial melting in mafic rocks. Contributions to Mineralogy and Petrology, 102, 281-297.

Morgan, G.B. VI and London, D. (1999) Crystallization of the Little Three layered pegmatite-aplite dike, Ramona District, California. Contributions to Mineralogy and Petrology, 136, 310-330.

Morgan, G.B. VI and London, D. (2005) Phosphorus distribution between potassic alkali feldspar and metaluminous haplogranite liquid at 200 MPa (H_2O): the effect of undercooling on crystal-liquid systematics. Contributions to Mineralogy and Petrology, 150, 456-471.

Mungall, J.E. (2002) Empirical models relating viscosity and tracer diffusion in magmatic silicate melts. Geochimica et Cosmochimica Acta, 66, 125-143.

Nash, W.P. and Crecraft, H.R. (1985) Partition coefficients for trace elements in silicic magmas. Geochimica et Cosmochimica Acta, 49, 2309-2322.

Neiva, A.M.R. (2014) Micas, feldspars and columbite-tantalite minerals from the zoned granitic lepidolite-subtype pegmatite at Namivo, Alto Ligonha, Mozambique. European Journal of Mineralogy, 25, 967-985.

Neves, L.J.P.F. and Godinho, M.M. (1999) Structural state of K-feldspar in some Hercynian granites from Iberia; a review of data and controlling factors. Canadian Mineralogist, 37, 691-700.

Parsons, I., Magee, C.W., Allen, C.M., Shelley, J.M.G., and Lee, M.R. (2009) Mutual replacement reactions in alkali feldspars II: trace element partitioning and geothermometry. Contributions to Mineralogy and Petrology, 157, 663–687.

Ren, M. (2004) Partitioning of Sr, Ba, Rb, Y, and LREE between alkali feldspar and peraluminous silicic magma. American Mineralogist, 89, 1290–1303.

Roda-Robles, E., Pesquera, A., Gil-Crispo, P., and Torres-Ruiz, J. (2012) From granite to highly evolved pegmatite: a case study of the Pinilla de Fermoselle granite-pegmatite system (Zamora, Spain). Lithos, 153, 192-207.

Roselieb, K. and Jambon, A. (1997)Tracer diffusion of potassium, rubidium, and cesium in a supercooled jadeite melt. Geochimica et Cosmochimica Acta, 61, 3101-3110.

Roy, B.N. and Navrotsky, A. (1984) Thermochemistry of charge-coupled substitutions in silicate glasses: the systems $M_{1/n}^{n+}AlO_2$-SiO_2 (M = Li, Na, K, Rb, Cs, Mg, Ca, Sr, Ba, Pb): Journal of the American Ceramic Society, 67, 606-610.

Royzenman, F.N. et al. (1982) Geochemical features and exploration value of various genetic types of biotite metasomatites in a rare-metal pegmatite field, International Geology Review, 24, 24-30, DOI: 10.1080/00206818209452363

Saasen, A., Jordal, O.H, Burkhead, D., Berg, P.C., Løklingholm, G., Pedersen, E.S, Turner, J., and Harris, M.J. (2002) Drilling HT/HP wells using a cesium formate based drilling fluid. Society of Petroleum Engineers, document SPE-74541-MS, https://doi.org/10.2118/74541-MS

Shannon, R.D. (1976) Systematic studies of interatomic distances in oxides. In The Physics and Chemistry of Minerals and Rocks (Strens, R.G.J., ed.). John Wiley & Sons, London, 403-431.

Shearer, C.K., Papike, J.J., Jolliff, B.L. (1992) Petrogenetic links among granites and pegmatites in the Harney Peak rare-element granite-pegmatite system, Black Hills, South Dakota. Canadian Mineralogist, 30, 785-809.

Smith, V.G. Tiller, T.P., and Rutter, J.W. (1955) A mathematical analysis of solute redistribution during solidification. Canadian Journal of Physics, 33, 723-744.

769 Stilling, A., Černý, P., and Vanstone, P.J. (2006) The Tanco pegmatite at Bernic Lake, Manitoba.
770 XVI. Zonal and bulk compositions and their petrogenetic significance. Canadian
771 Mineralogist, 44, 599-623.
772 Teerstra, D.K., Černý, P., and Hawthorne, F.C. (1999) Geochemistry and petrology of late K-
773 and Rb- feldspars in the Rubellite pegmatite, Lilypad Lakes, NW Ontario. Canadian
774 Mineralogist, 65, 237-247.
775 Volfinger, M., (1969) Partage de Rb et Cs entre sanidine, muscovite et solution a 600° C, 1,000
776 bars. Comptes Rendus Hebdomadaires des Seances de l'Academie des Sciences, Serie D:
777 Sciences Naturelles, 269, 1-3.
778 Webster, J.D., Holloway, J.R., and Hervig, R.L. (1989) Partitioning of lithophile trace elements
779 between H_2O and $H_2O + CO_2$ fluids and topaz rhyolite melt. Economic Geology, 84, 116-
780 134.
781

782 **Captions to figures**

783 **Figure 1.** A Rayleigh model of the K/Cs ratio of K-feldspars versus Cs in K-feldspar, and data
784 for individual pegmatites in Rwanda from Hulsbrosch et al. (2014). The labels for the types of
785 pegmatites are from Hulsbosch et al. (2014). Modeled curves (green) show the K/Cs ratios in K-
786 feldspar and in melt. The fraction of melt crystallized, 1-F, is denoted at three values on the
787 curve for K/Cs in feldspar. See the text for the parameters of the Rayleigh model.
788 **Figure 2.** A plot of K/Cs in K-feldspar versus depth in the holes that represent three oblique
789 intersections from margin to margin across a single dike, the General Electric Southeast, near
790 Buckfield, Maine.

Figure 3. A Rayleigh model (green) of K/Cs in melt and in K-feldspar, and K/Cs ratios of feldspars from two pegmatite dikes near Ramona, California, plotted against 1-F, fraction of melt crystallized. See the text for details of the Rayleigh model. For the Swamp dike, two outlier values are illustrated in lighter blue.

Figure 4. (a) Rayleigh models of the K/Cs ratio of K-feldspars crystallized simultaneously from melt (blue) and aqueous solution (green) versus the fraction of melt crystallized for the condition of $D_{Cs}^{aq/melt} = 0.2$, wherein Cs is highly compatible in melt compared to aqueous solution. **(b)** Rayleigh models of the K/Cs ratio of K-feldspars crystallized simultaneously from melt (blue) and aqueous solution (green) versus the fraction of melt crystallized for the condition of $D_{Cs}^{aq/melt} = 6.0$, wherein Cs is highly compatible in aqueous solution compared to melt.

This is the peer-reviewed, final accepted version for American Mineralogist, published by the Mineralogical Society of America.
The published version is subject to change. Cite as Authors (Year) Title. American Mineralogist, in press.
DOI: https://doi.org/10.2138/am-2021-7855. http://www.minsocam.org/

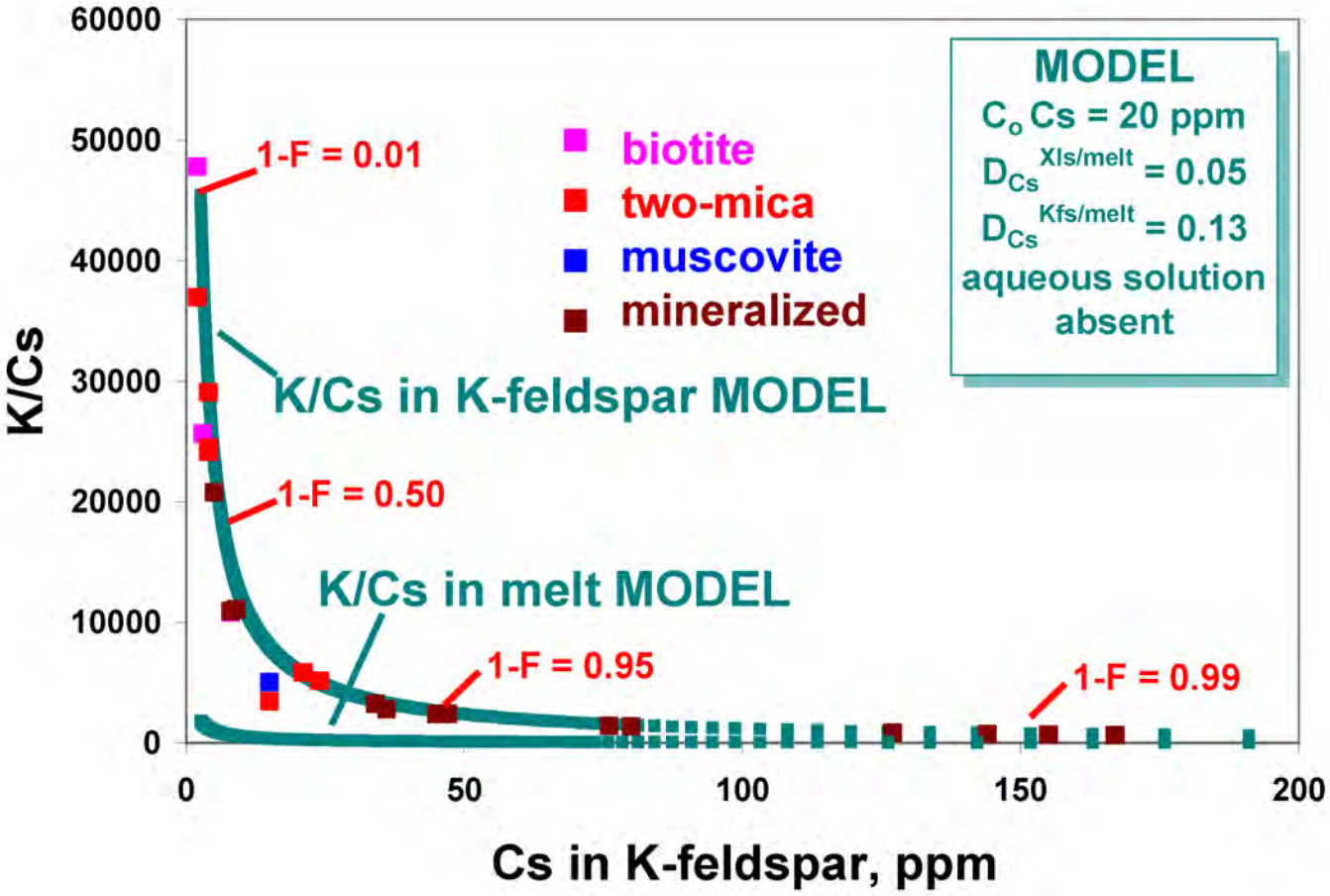

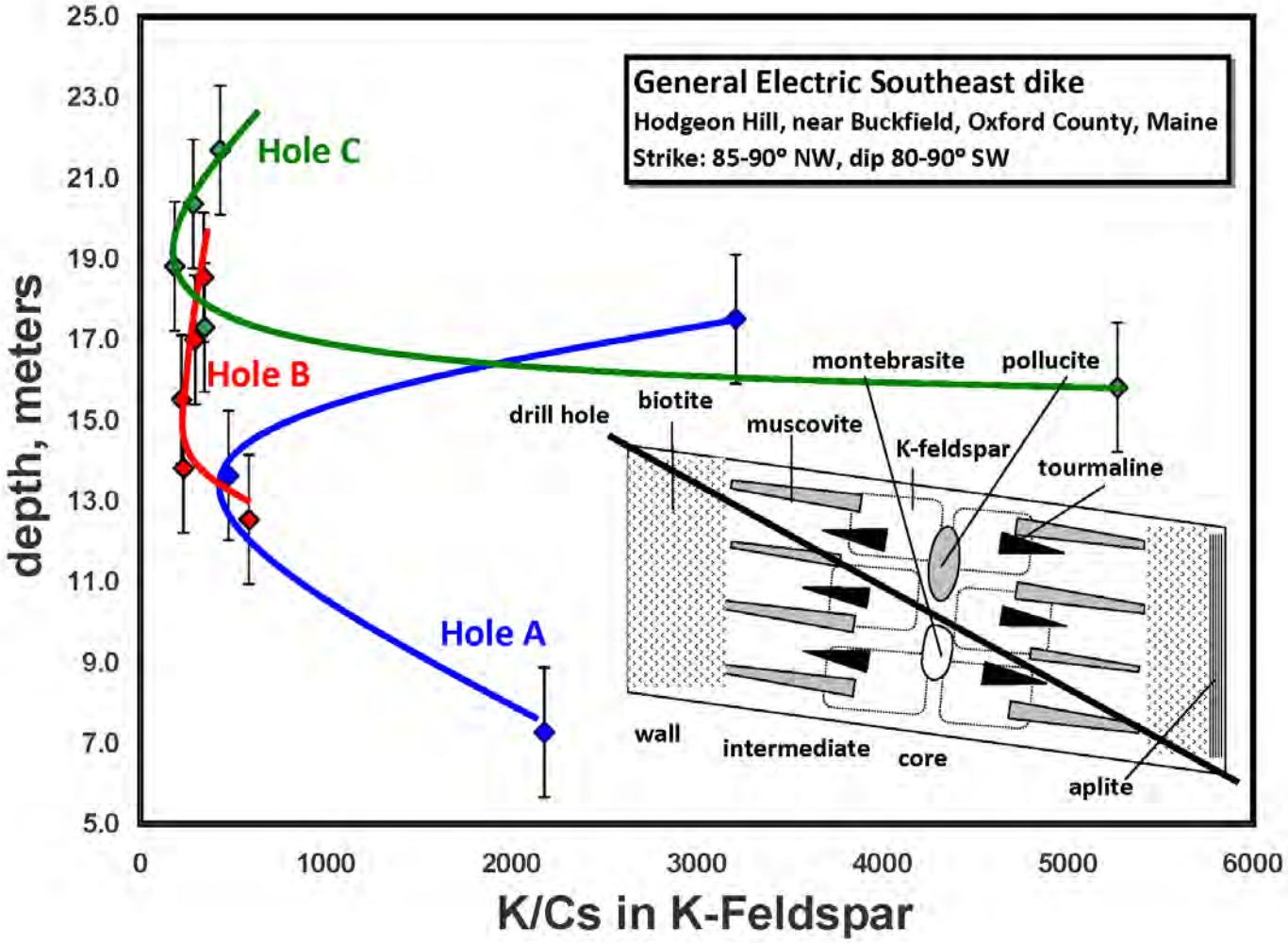

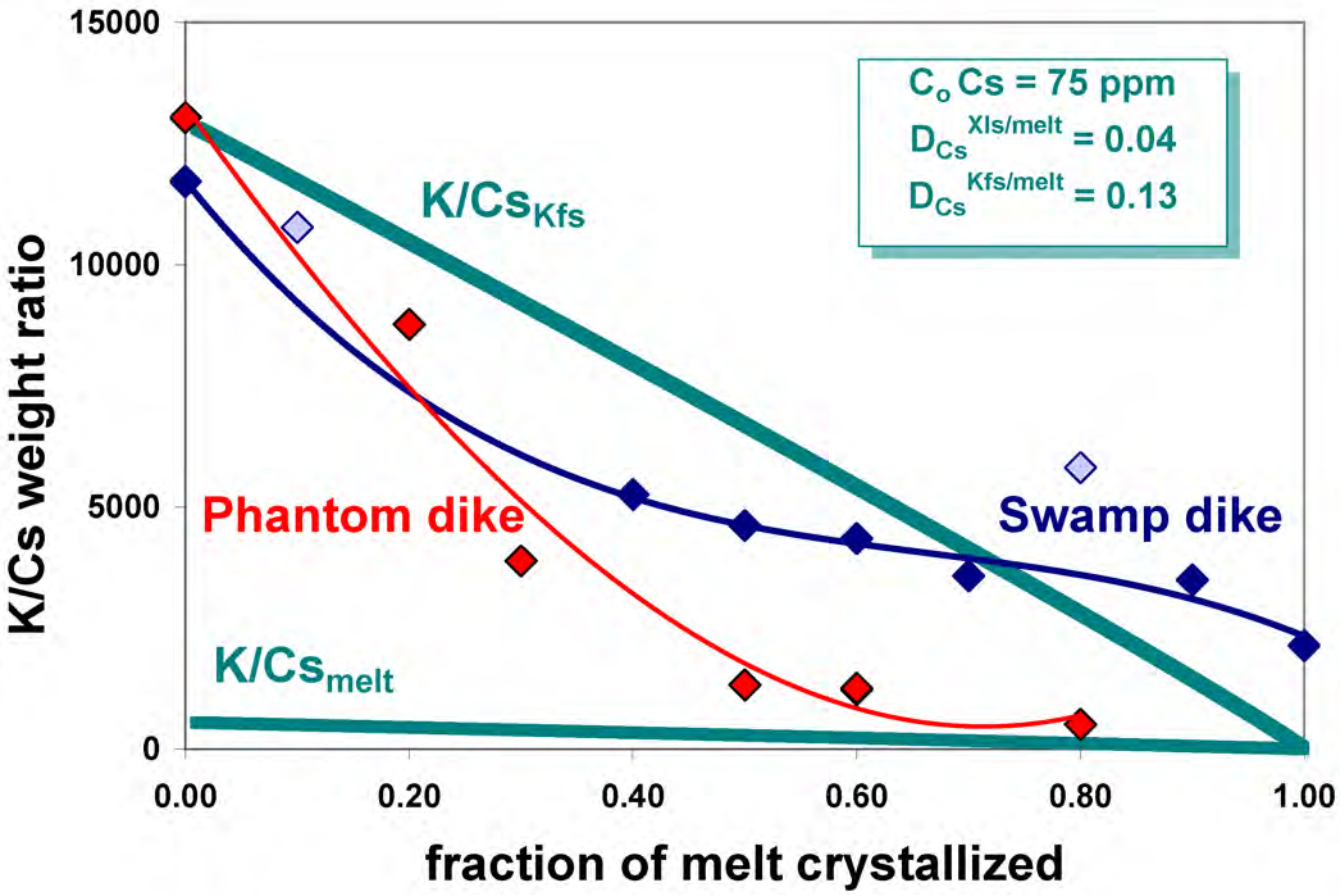

This is the peer-reviewed, final accepted version for American Mineralogist, published by the Mineralogical Society of America.
The published version is subject to change. Cite as Authors (Year) Title. American Mineralogist, in press.
DOI: https://doi.org/10.2138/am-2021-7855. http://www.minsocam.org/

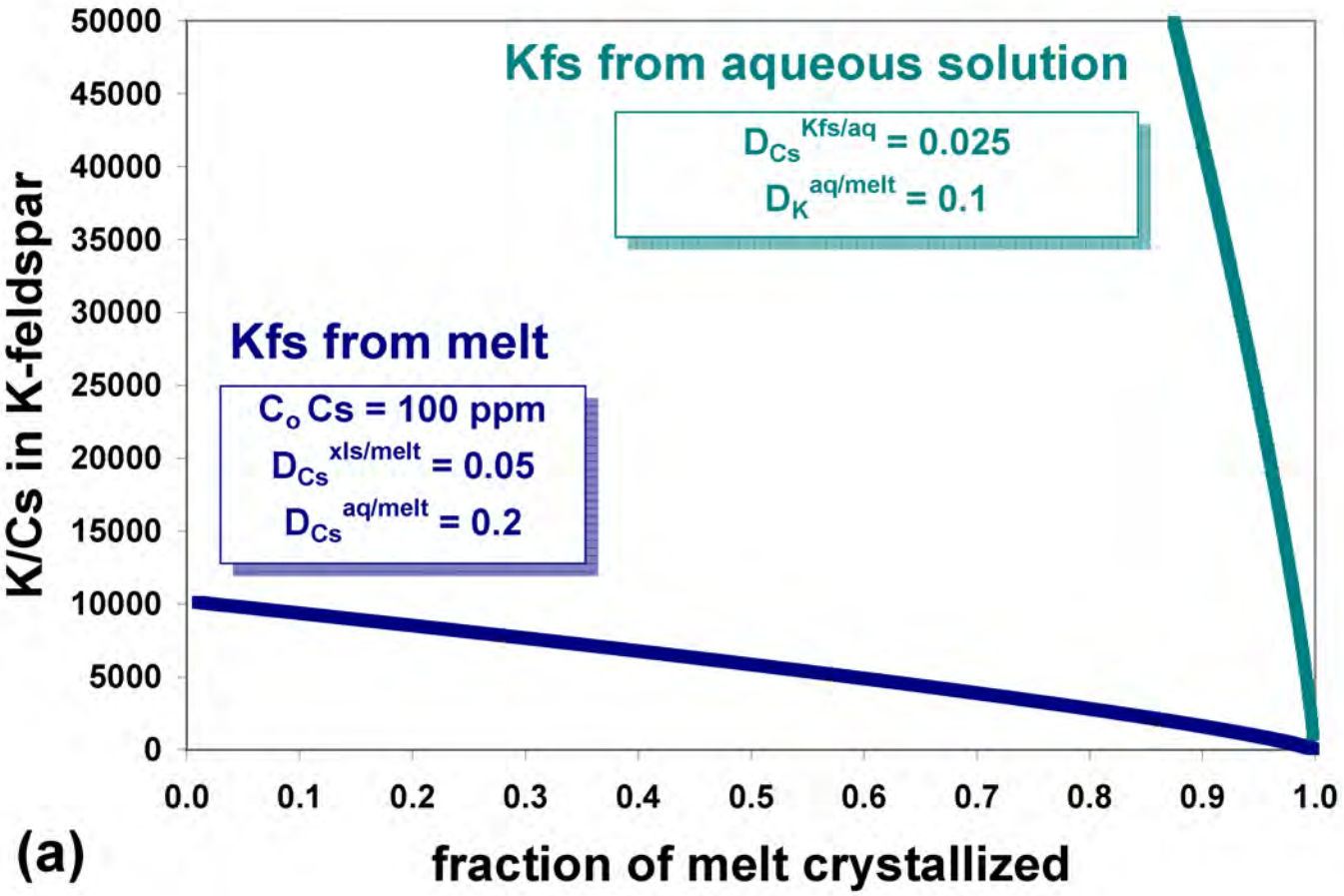

This is the peer-reviewed, final accepted version for American Mineralogist, published by the Mineralogical Society of America.
The published version is subject to change. Cite as Authors (Year) Title. American Mineralogist, in press.
DOI: https://doi.org/10.2138/am-2021-7855. http://www.minsocam.org/

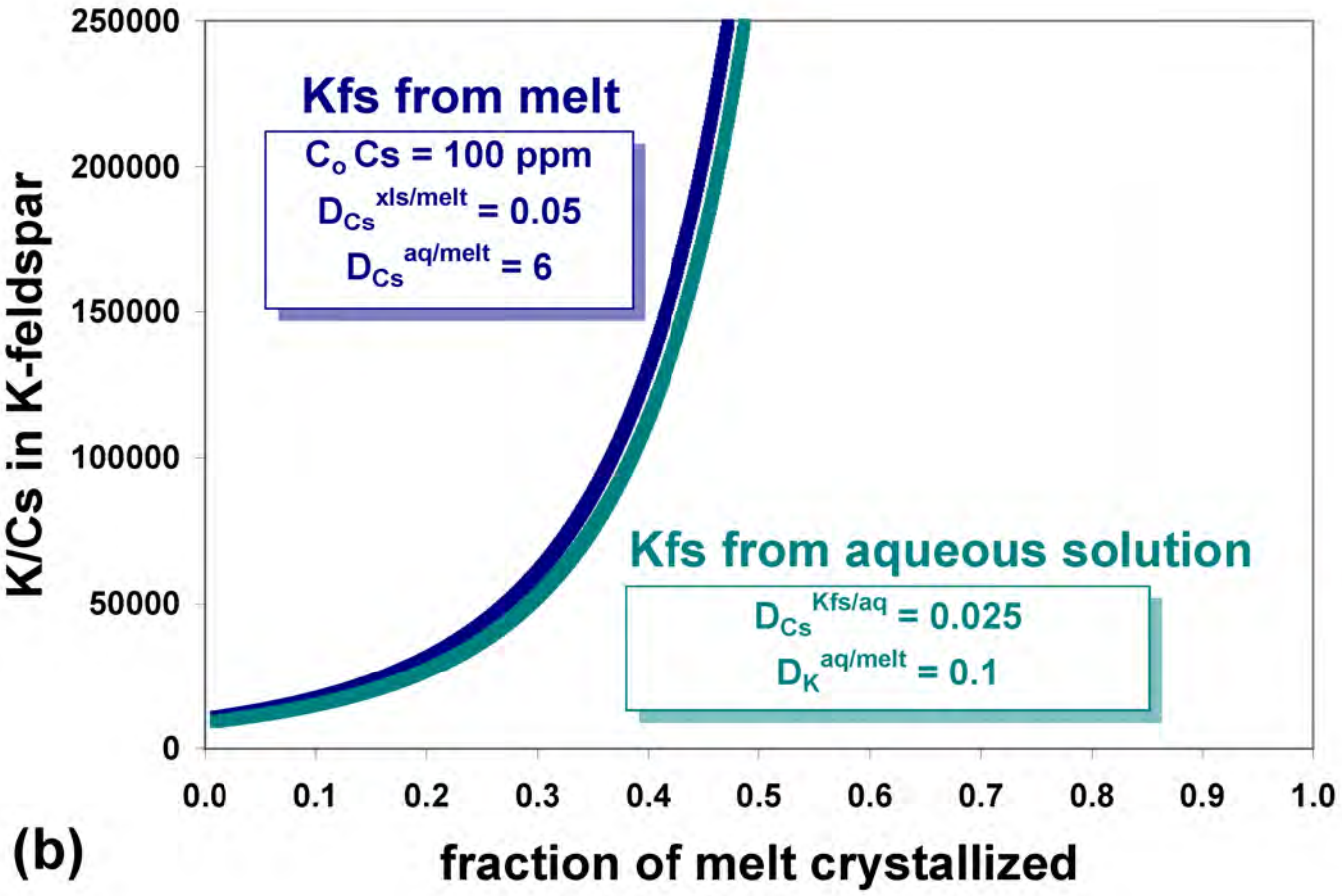

(b)

This is the peer-reviewed, final accepted version for American Mineralogist, published by the Mineralogical Society of America.
The published version is subject to change. Cite as Authors (Year) Title. American Mineralogist, in press.
DOI: https://doi.org/10.2138/am-2021-7855. http://www.minsocam.org/

Table 1. Rayleigh model parameters

Granite Bulk Distribution Coefficients

	mode	D(K)	fraction[1]
Qtz	0.33	0.00	0.00
Pl	0.36	0.50	0.18
Kfs	0.24	2.38	0.57
Bt	0.02	2.47	0.05
Ms	0.05	2.40	0.12
		D =	**0.92**

	mode	D(Cs)[2]	fraction
Qtz	0.33	0.00	0.00
Pl	0.36	0.00	0.00
Kfs	0.24	0.13	0.03
Bt	0.02	0.30	0.01
Ms	0.05	0.20	0.01
		D =	**0.05**

Pegmatite Bulk Distribution Coefficients

	mode	D(K)	fraction
Qtz	0.34	0.00	0.00
Pl	0.32	0.50	0.16
Kfs	0.28	2.52	0.83
Bt	0.00	2.40	0.00
Ms	0.06	2.40	0.02
		D =	**1.01**

	mode	D(Cs)	fraction
Qtz	0.34	0.00	0.00
Pl	0.32	0.00	0.00
Kfs	0.28	0.13	0.04
Bt	0.00	0.30	0.00
Ms	0.06	0.20	0.00
		D =	**0.05**

[1] the weighted contribution of each mineral to the bulk distribution coefficient, D

[2] from Table 10-2 of London (2008).